

# Seismic analysis of the stability of a deep geological repository in sedimentary rock

Z. Fu, E. Evgin, & J.A. Infante Sedano

*Department of Civil Engineering – University of Ottawa, Ottawa, Ontario, Canada*

S. Sivathayalan

*Department of Civil Engineering – Carleton University, Ottawa, Ontario, Canada*



2011 Pan-Am CGS  
Geotechnical Conference

## ABSTRACT

A numerical analysis is conducted to determine the intensity of damage in Cobourg limestone around a deep geological repository. The extent of the damage and its effect on the fluid flow properties of the rock mass are determined by using a coupled hydro-mechanical distinct element analysis. The results include the magnitude of displacements at potentially critical locations, stress distribution around the emplacement rooms, the changes in the permeability around the repository, relative tangential movements along the bedding planes and the aperture opening and closing. The geostatic and seismic loads are considered to explore the performance of the repository.

## RÉSUMÉ

Une analyse numérique a été effectuée afin de déterminer l'intensité des dommages dans de la roche calcaire de Cobourg autour d'un entrepôt géologique profond. L'étendue des dommages et ses effets sur les propriétés de flux des fluides dans la masse rocheuse sont déterminés en utilisant la méthode des éléments distincts et un modèle hydromécanique couplé. Les résultats comprennent l'amplitude des déplacements et les zones critiques potentielles, la distribution des contraintes autour des chambres de stockage, les changements de perméabilité autour de l'entrepôt, les mouvements tangentiels relatifs le long des plans de stratification et la formation et la clôture des ouvertures. Les charges géostatiques et sismiques sont aussi considérées afin d'explorer la performance de l'entrepôt.

## 1 INTRODUCTION

Radioactive waste disposal in deep geological repositories (DGR) is currently being considered in many countries. In Canada, one of the proposed repositories is to be located within an Ordovician sedimentary rock formation in southern Ontario (Hatch Limited 2008). The depth to the repository is about 680 m below the ground surface. The design of these types of facilities requires a coupled analysis of thermal, hydrological, mechanical, and chemical (THMC) processes. Once the repository is excavated, the pre-existing discontinuities in the rock can close or open. It is also possible that new fractures might initiate, coalesce and propagate. In general, excavations cause damage to the rock in the vicinity of the openings. As a result, the characteristics of the rock mass are altered. Therefore, it is necessary to know the size of the excavation damaged zone (EDZ) and the intensity of damage at all locations within the EDZ. The damage is largest near the walls of the repository and its negative effect reduces with increasing distance from the repository.

In order to predict the performance of underground repositories, the modeling of the coupled processes in the geological media, such as a jointed rock mass, is required. In addition, the numerical results need to be verified using field tests. For example, the ongoing international DECOVALEX Project deals with the development of numerical models and their validation by field testing in underground research laboratories (Jing et al 1996). The results of DECOVALEX Project have

contributed greatly to our understanding of the coupled processes and the requirements for mathematical models. Both the continuum and discrete element methods have been used in the numerical analyses (Noorishad and Tsang 1996). Analytical and numerical solutions using the continuum approach (Bai and Elsworth 2000) produced results on the deformation, fluid flow, and transport characteristics of geological materials with emphasis given to the coupled processes. Due to the presence of discontinuities such as bedding planes and joints, sedimentary rocks behave as anisotropic materials. Anisotropic rock mass behaviour is controlled by planes of weaknesses. For example, the influence of anisotropy on the stability of excavations is shown by Bewick and Kaiser (2009). Shen and Barton (1997) used Universal Distinct Element Code (UDEC) to study the excavation disturbed zones around underground openings in jointed rock mass. Tonon (2004) investigated the effects of elastic anisotropy on the plane strain behaviour of the underground structures. However, the continuum approach does not simulate relative tangential movements along discontinuities.

In the present study, UDEC is utilized to perform the numerical analysis. Measured geotechnical properties of various rock layers are used as input to the numerical model. The hydro-mechanical coupling in the analysis of the repository is simulated and its influence on the characteristics of EDZ is examined. The effect of the excavation of multiple emplacement rooms on the amount of damage in the rock mass is also investigated. The effects of both static and seismic loading are considered.

## 2 SEDIMENTARY ROCKS OF SOUTHERN ONTARIO

Sedimentary rocks are formed from compaction, cementation of sediments or precipitation of crystal aggregates (e.g., shale, siltstone, sandstone, and limestone). In general, sedimentary rocks are cross-anisotropic geomaterials which exhibit isotropic behavior along bedding planes but anisotropy in the planes perpendicular to the bedding planes (Lo and Hefny, 1999). In addition, high horizontal stresses are prevalent in the sedimentary rock formations in southern Ontario. The field test data show that the conservative value of in-situ stress ratio ( $\sigma_H/\sigma_v$ ) is about 1.2 to 2 at the DGR level (Lam et al. 2007) and the permeability in the horizontal direction at the location of the repository is ten times higher than the permeability in the vertical direction.

## 3 NUMERICAL ANALYSIS OF THE STABILITY OF A DGR IN SEDIMENTARY ROCK

The analysis is carried out separately for a single emplacement room and for two emplacement rooms.

### 3.1 Geometry of a Single Emplacement Room and Analysis Domain

A rectangular emplacement room of 8.6 x 7.0 meters is excavated 676 meters (the depth to the top of the emplacement room) below the ground surface. A cross section of the analysis domain is shown in Figure 1. It is assumed that the room is unsupported. Boundary conditions used in the analysis are as follows: the bottom surface of the domain is constrained in the vertical direction and no horizontal movement is allowed at the two vertical sides of the rock mass in the static analysis. The horizontal stress versus vertical stress ratio,  $K_0$ , is set to 1.5.

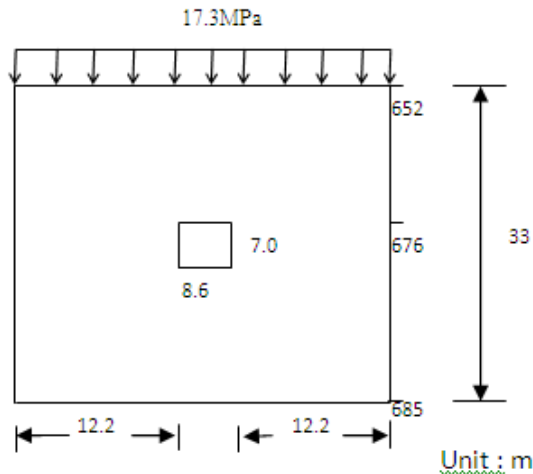


Figure1. Schematics of solution region

### 3.2 Parameters for Jointed Rock Model and Joint Hydraulic Properties

The parameters for the jointed rock model are listed in Table1. The thickness of the bedding plane is chosen 1 meter. The joint sets are used in the distinct element analysis to represent the orientation of bedding planes ( $\Psi$ ) as shown in Figure 2. A bedding plane  $\Psi = 0^\circ$  was used to represent the most likely orientation at the proposed location. The joint hydraulic conductivity used in this study is  $10^{-13}$  m/s, which is based on the measured value of hydraulic conductivity in the rock units at the proposed repository location.

The analysis is performed for undrained conditions. Plane strain state was assumed. Deformable blocks are used in the simulations.

Table1. Parameters for jointed rock model (Itasca, 2008)

Bulk modulus (GPa)	K	19.38
Shear modulus (GPa)	G	15.14
Joint normal stiffness (GPa/m)	jkn	160.3
Joint tangent stiffness (GPa/m)	jks	80.1
Joint cohesion (MPa)		38.3
Joint friction angle (degree)		35
Joint tensile strength (MPa)		15.3

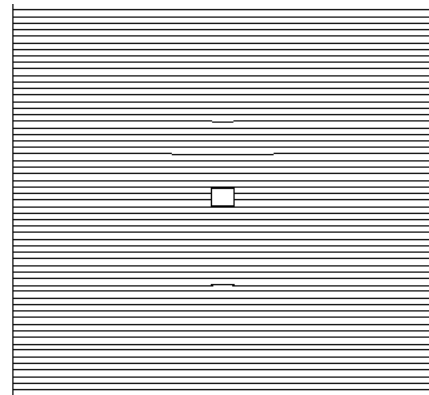


Figure 2. Schematic view of 2D model showing the bedding plane orientation (Assumed value:  $\Psi = 0^\circ$ )

### 3.3 Numerical Analysis

The previous studies show that the orientation of bedding planes has a substantial effect on the deformations and stability of the emplacement rooms and the damage in the rock is strongly influenced by the values of  $K_0$  (Evgin and Fu 2009). In this study, the influence of some other factors such as fluid boundary conditions, construction stages and dynamic loading on EDZ is investigated. In order to explore the effects of each factor on the EDZ, the numerical results are produced for the magnitude of displacements at potentially critical locations, stress distribution around the emplacement room, relative tangential movements along the bedding planes and the aperture opening and closing.

### 3.3.1 Analysis of Hydro-mechanical Processes

In order to explore the influence of hydro-mechanical coupling (HM) on EDZ around the emplacement room, two types of numerical analyses are performed. In one of the analyses, only the mechanical process (M) without pore water pressure is considered. The second analysis is performed for fully coupled hydro-mechanical processes (HM).

Shear displacements in the joints resulting from the excavation of the emplacement room are presented in Figure 3. The largest shear displacements take place at the corners of the room in both types of analysis. The magnitude of the maximum shear displacement is 0.0056 m in the HM analysis and 0.005m in the M analysis.

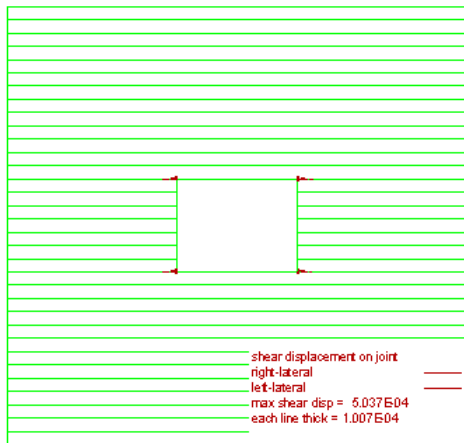


Figure 3. Joint shear displacements after excavation

Figure 4 shows the displacement vectors in the rock mass around the emplacement room after the excavation. The Largest horizontal displacements take place in joints passing through the springlines of the room. The magnitude of the maximum displacement is 0.017 m in the HM analysis and 0.012 m in the M analysis.

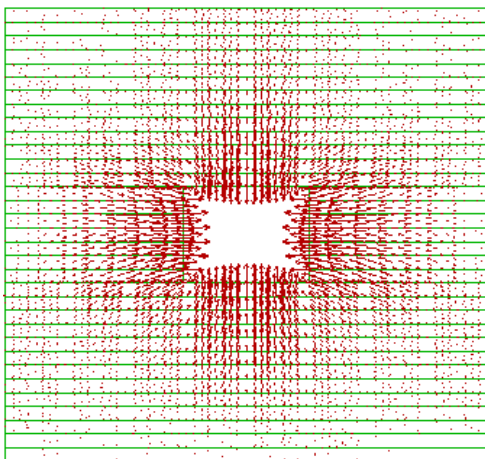
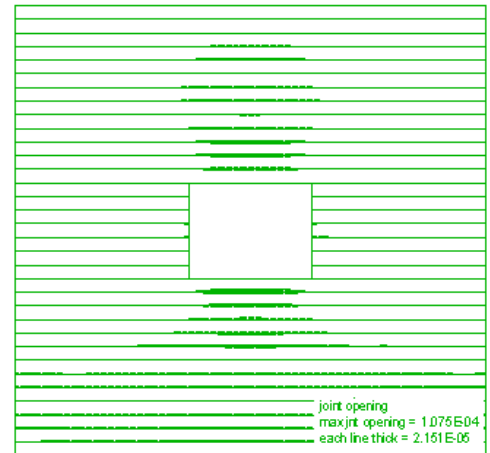
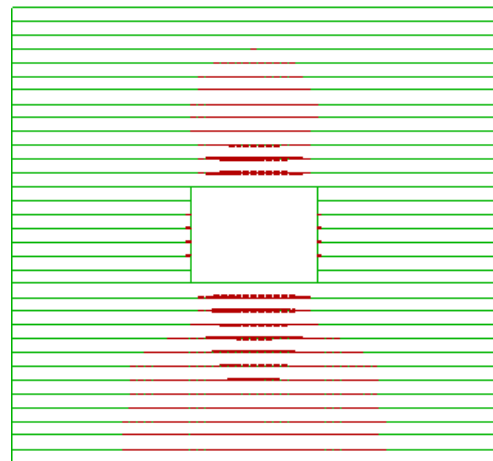


Figure 4. Displacement vectors around the emplacement room after the excavation

The separation of joints at the end of the excavation of the emplacement room is illustrated in Figure 5. The damage due to joint separation occurs above the crown and below the invert of the room in shaded areas. HM analysis produced a larger damaged area than that of M analysis. However, the calculated value of the maximum joint separation was 0.0011 m in the M analysis and 0.00085 m in the HM analysis.



(a) M Analysis

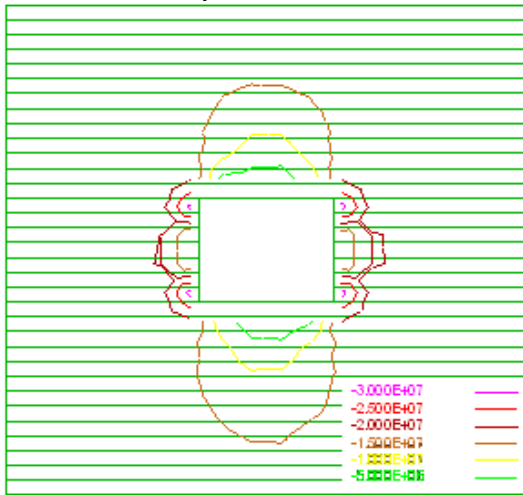


(b) HM Analysis

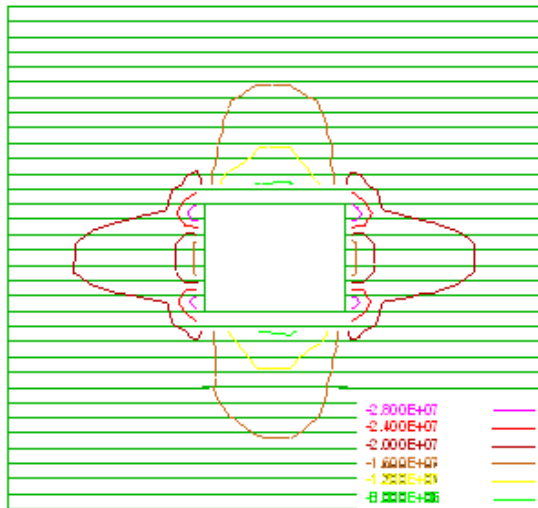
Figure 5. Joint separation after excavation

The vertical stress distribution around the excavation is presented in Figure 6. The way in which the initial in-situ vertical stresses are redistributed due to excavation is different in the M and HM analyses. Although, the largest vertical stresses are concentrated at the corners of the room in both analyses, HM analysis produced a greater influence of excavation on the redistribution of vertical

stresses. The affected area is larger in the HM analysis than that of the M analysis.



(a) M Analysis



(b) HM Analysis

Figure 6. Vertical stress contours after excavation

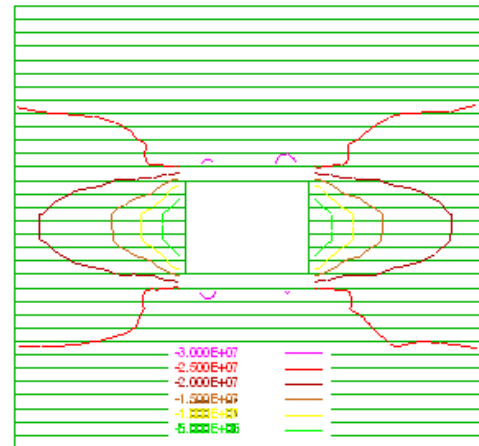
Horizontal stress distribution around the excavation is presented in Figure 7. In the HM analysis, the stress redistribution takes place in a larger area above the crown and below the invert than those of the M analysis.

The calculated values of the stresses and pore water pressures at Point 1 (1 meter above the center of crown) and Point 2 (1 meter away in the horizontal direction from the spring-lines) before and after excavation are presented in Table 2. It can be seen that after the excavation, the pore water pressures and normal stresses in the rock mass above the crown decreased. However, the shear stresses increased by a large amount. On the other hand, the shear stresses in the rock mass besides the spring-line of the room decreased. There is only a small change in the pore water pressures and normal stresses in this zone.

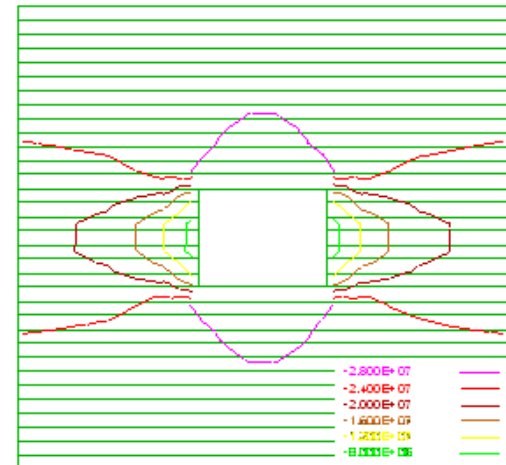
Table 2. The calculated values of stresses and pore water pressures before and after excavation

POINT	NORMAL STRESS (kPa)		SHEAR STRESS (kPa)		PORE WATER PRESSURE (kPa)	
	Before	After	Before	After	Before	After
1	1.38e7	8.5e6	2.06e7	2.65e7	6.6e6	5.1e6
2	1.77e7	2.14e7	2.23e7	1.61e7	6.6e6	6.5e6

Meanwhile, the rock mass permeability around the emplacement room also changed. For instance, the permeability of rock mass in Zone1 increased by about 9 % at a point 5 meters above the crown as shown in Figure 8. Zone1 is located at the joint separation area where effective stresses decreased. However, the permeability in Zone 2 next to the vertical walls of the room decreased by about 3 %. The increase in the effective stresses in Zone 2 leads to the reduction in the permeability of rock mass.



(a) M Analysis



(b) HM Analysis

Figure 7. Horizontal stress contours after excavation

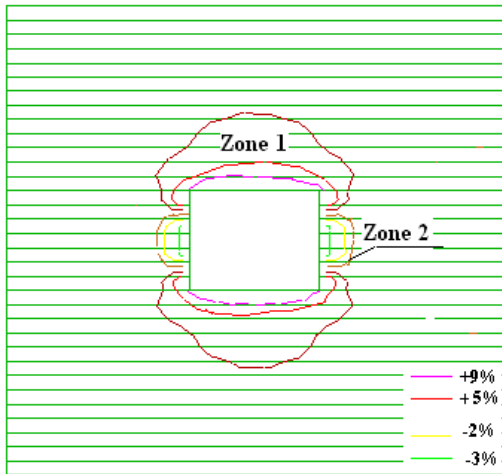
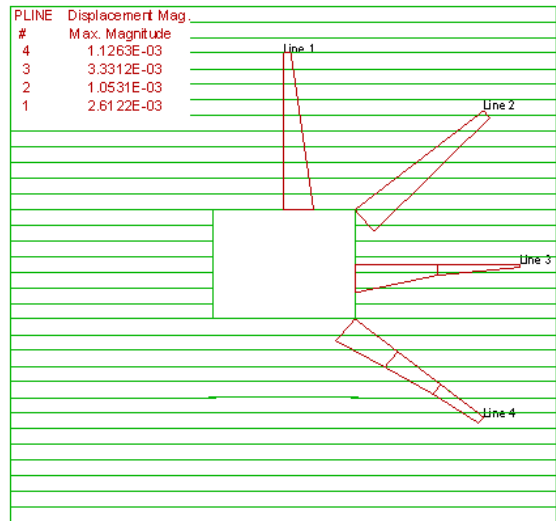


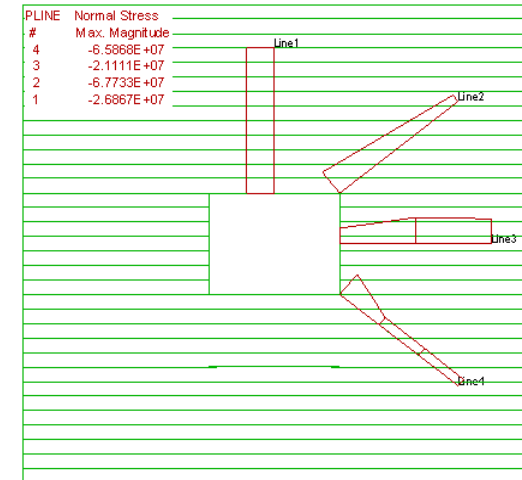
Figure 8. Permeability distributions after excavation

Line 1, 2, 3, 4 are used to present some numerical results. Line 1 is vertical and starts at the center of the crown. Line 3 is horizontal and begins at the springline. Line 2 and Line 4 start at the corners of the room. Distributions of displacements, normal stresses and shear stresses along the lines 1, 2, 3, 4 are shown in Figures 9, 10, and 11. It can be seen that large displacements take place at the crown and springline (Figure 9). Figures 10 and 11 indicate that the stresses are concentrated at the corners of the room in both normal and shear stress values.

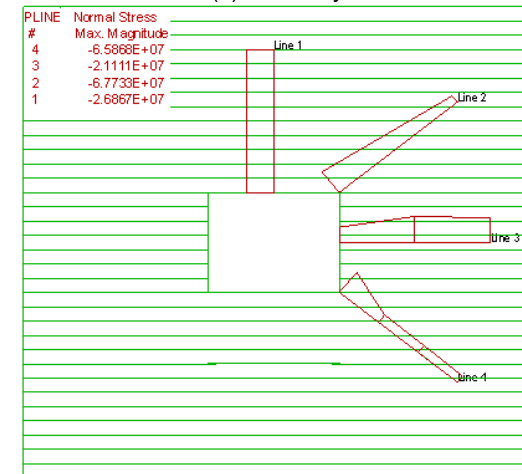


(b) HM Analysis

Figure 9. Distributions of displacements along Line 1, 2, 3, 4

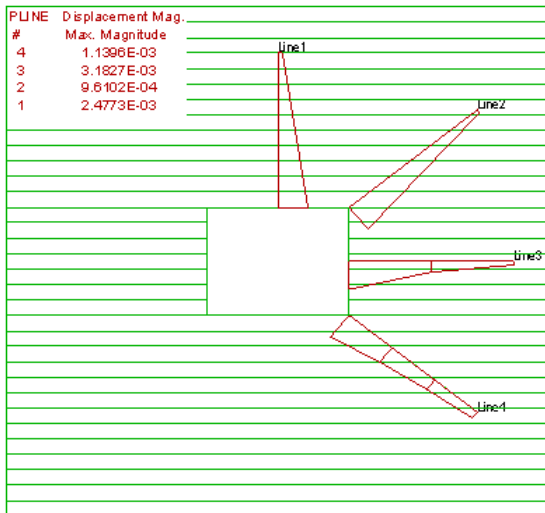


(a) M Analysis

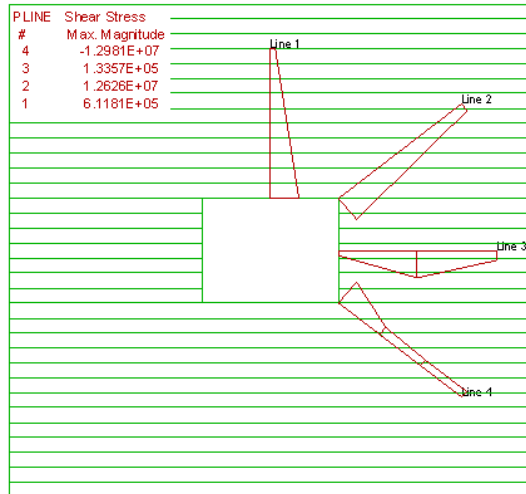


(b) HM Analysis

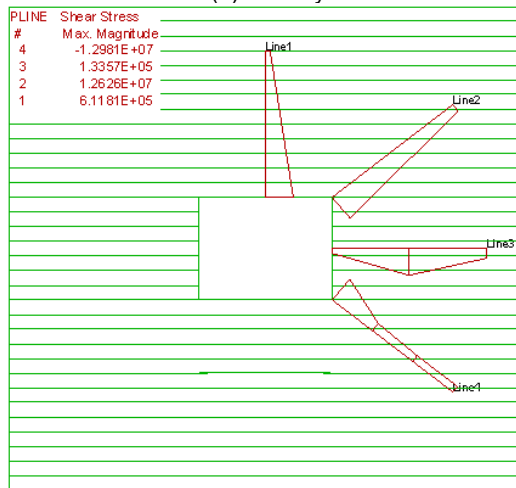
Figure 10. Distributions of normal stresses along Line 1, 2, 3, 4



(a) M Analysis



(a)M Analysis



(b) HM Analysis

Figure 11. Distributions of shear stresses along Line 1, 2, 3, 4

### 3.3.2 Effect of Second Emplacement Room on EDZ

A second room which is 17.2 m away from the first room is included in the analysis. The size of the EDZ is investigated. The stresses and displacements around the two emplacement rooms and the pillar are determined.

The major joint shear displacements take place starting from near the right springline of the first room and progress into the pillar. The maximum shear displacement occurs in the pillar as shown in Figure 12.

The principal stresses are redistributed after the excavation. For example, the values of the minor principal stress are reduced along a horizontal line passing through the spring line of the rooms which includes the rock forming the pillar as shown in the Figure 13.

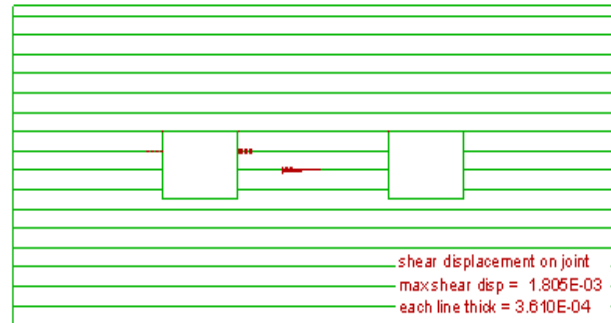


Figure 12 Joint shear displacements around two emplacement rooms

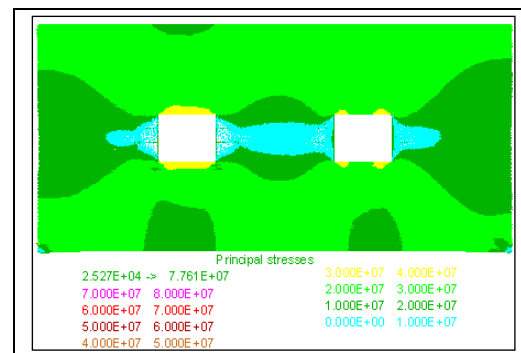


Figure 13 Minor principal stress distribution around two emplacement rooms

### 3.3.3 Seismic Analysis of One Room

A seismic analysis is necessary to determine the size of EDZ around the DGR and to establish the severity of damage in the rock mass. In the analysis, a seismic load is applied after the rock mass reached an equilibrium stage at the end of the excavation. A sinusoidal shear wave and a viscous boundary condition are applied to the base of the model. Free-fields are created at the lateral boundaries to prevent the outward-propagating waves from reflecting back into the model.

The calculated values of the maximum shear displacement, maximum joint opening, stresses and displacements at the crown and at the spring-line for each cycle of loading are presented in Table 3. The following abbreviations are used in the table. MJSD= Maximum joint shear displacement (m); ESSD= Extent of significant shear displacement (m); JS= Joint separation (m); VDC= Vertical displacement at the crown (m); HDSL= Horizontal displacement at the spring-line (m); NSSL= Normal stress ( $s_{yy}$ ) at the spring-line (Pa); NSC= Normal stress ( $s_{xx}$ ) at the crown (Pa).

It can be seen in Table 3 that the effect of seismic loading on the joint shear displacements (MJSD) and joint separations (JS) is very large.

Table 3. The calculated values of displacements and stresses in static and seismic analysis

	Seismic	Static
MJSD(m)	0.0591	0.005
ESSD(m)	41	10
JS(m)	0.0014	0.001
VDC(m)	0.017	0.014
HDSL(m)	0.029	0.016
NSSL(Pa)	8.07e6	4.5e6
NSC(Pa)	0.95e7	0.74e7

The extent of significant shear displacement (ESSD) in the seismic analysis is four times bigger than that in static analysis. The damaged zone of rock mass is expanding further during the seismic loading as shown in Figure14. The EDZ extends in the horizontal direction. The displacement of rock mass at the crown of the cavern is 1.4 times that of static analysis. Moreover, the size of the damaged area is increasing with the additional cycles of loading.

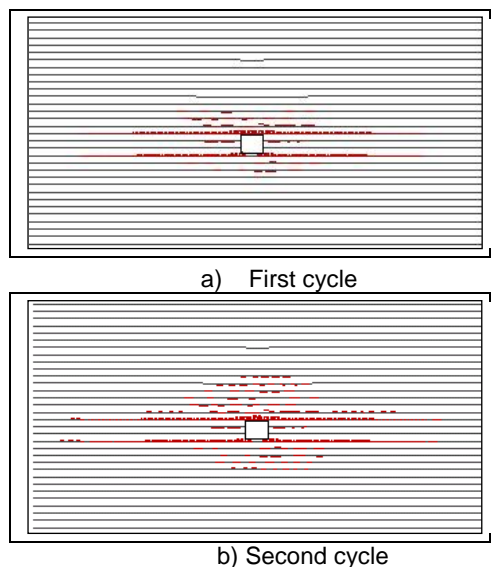


Figure14. Failure zones in the rock mass around the emplacement room with loading cycles

#### 4 CONCLUSIONS

- 1) The hydro-mechanical processes have more effect on the deformations and stability of emplacement rooms than the mechanical processes alone.
- 2) The size of the damaged zone around the emplacement rooms is enlarged significantly by seismic loading.
- 3) The excavation of the second room extends the excavation damaged zone of the first room horizontally; the maximum shear displacement occurs in the pillar.
- 4) The permeability of the rock mass increases in the

areas above the crown but it decreases next to the springlines.

#### ACKNOWLEDGEMENTS

The financial support for this investigation was provided by the Natural Sciences and Engineering Research Council of Canada.

#### REFERENCES

- Bai, M. and Elsworth, D. (2000). *Coupled Processes in Subsurface Deformation, Flow, and Transport*. ASCE Press.
- Bewick, R.P. and Kaiser, P.K. 2009. Influence of rock mass anisotropy on tunnel stability. *ROCKENG09, Proceedings of the 3<sup>rd</sup> CANUS Rock Mechanics Symposium*, Toronto, May 2009, Paper #3995.
- Evgin, E. and Fu, Z. 2009. Distinct element and finite element analyses of underground excavations in jointed rock mass. *Canadian Geotechnical Conference*, Halifax, 2009, Paper #3995
- Hatch Limited. 2008. *Supporting technical report – Geomechanical modeling*. OPG'S deep geologic repository for low and intermediate level waste conceptual design study. May 2008, p252.
- Itasca Consulting Group, Inc. 2008. *Supporting technical report –Phase I Long-Term Cavern Stability*. OPG'S deep geologic repository for low and intermediate level waste. November 2008, p69.
- Universal Distinct Element Code*, version 4.0, user's guide.
- Jing, L., Tsang, C.F., Stephansson, O., and Kautsky, F. 1996. Validation of Mathematical Models against Experiments for Radioactive Waste Repositories – DECOVALEX Experience. *Coupled Thermo-Hydro-Mechanical Processes of Fractured Media, Developments in Geotechnical Engineering*, Vol. 79. Elsevier Science B.V. (TS 898 .C68 1996).
- Jing, L., and Feng, X. 2003. Numerical modeling for coupled thermo-hydro-mechanical and chemical processes (THMC) of geological media—international and Chinese experiences. *Chinese journal of rock mechanics and engineering*. 22(10), 1704-1715.
- Lam, T., Martin, D., and McCreath, D. 2007. Characterising the geomechanics properties of the sedimentary rocks for the DGR excavations. *Canadian Geotechnical Conference*, Ottawa 2007, pp. 636-644.
- Lo, K.Y. and Hefny, A.M. 1999. Basic rock mechanics and testing. *Geotechnical and Geoenvironmental Engineering Handbook*. Kluwer Academic Publisher 1999.147-172.
- Noorishad, J., and Tsang C.F. 1996. Coupled thermo-hydro-elasticity phenomena in variably saturated fractured porous rocks -- formulation and numerical solution. *Elsevier*, 1996, 93-134.
- Shen, B. and Barton, N. 1997. The disturbed zone around tunnels in jointed rock masses. *Int. J. Rock Mechanics and Mining Sciences*. Vol. 34, No. 1, pp. 117-125.
- Tonon, F. 2004. Does elastic anisotropy significantly affect a tunnel's plane strain behaviour? *Journal of the Transportation Research Board*, No.1868, 156-168.